Kindlin-3 regulates integrin activation and adhesion reinforcement of effector T cells

Federico A. Moretti[a,1], Markus Moser[a,1], Ruth Lyck[b], Michael Abadier[b], Raphael Ruppert[a], Britta Engelhardt[b], and Reinhard Fässler[a,2]

[a]Department of Molecular Medicine, Max Planck Institute of Biochemistry, D-82152 Martinsried, Germany; and [b]Theodor Kocher Institute, University of Bern, CH-3012 Bern, Switzerland

Edited by Timothy A. Springer, Immune Disease Institute, Program in Cellular and Molecular Medicine, Children's Hospital Boston, Boston, MA, and approved September 10, 2013 (received for review August 28, 2013)

Activated T cells use very late antigen-4/α4β1 integrin for capture, rolling on, and firm adhesion to endothelial cells, and use leukocyte function-associated antigen-1/αLβ2 integrin for subsequent crawling and extravasation. Inhibition of α4β1 is sufficient to prevent extravasation of activated T cells and is successfully used to combat autoimmune diseases, such as multiple sclerosis. Here we show that effector T cells lacking the integrin activator Kindlin-3 extravasate and induce experimental autoimmune encephalomyelitis in mice immunized with autoantigen. In sharp contrast, adoptively transferred autoreactive T cells from Kindlin-3–deficient mice fail to extravasate into the naïve CNS. Mechanistically, autoreactive Kindlin-3–null T cells extravasate when the CNS is inflamed and the brain microvasculature expresses high levels of integrin ligands. Flow chamber assays under physiological shear conditions confirmed that Kindlin-3–null effector T cells adhere to high concentrations of vascular cell adhesion molecule-1 and intercellular adhesion molecule-1, albeit less efficiently than WT T cells. Although these arrested T cells polarize and start crawling, only few remain firmly adherent over time. Our data demonstrate that the requirement of Kindlin-3 for effector T cells to induce α4β1 and αLβ2 integrin ligand binding and stabilization of integrin–ligand bonds is critical when integrin ligand levels are low, but of less importance when integrin ligand levels are high.

integrin affinity | EAE

In experimental autoimmune encephalitis (EAE), autoreactive $CD4^+$ Th cells, which recognize components of the myelin sheath of nerve fibers, extravasate into the CNS and induce breakdown of the blood–brain barrier and severe inflammation, leading to the destruction of brain tissue (1). Integrins play pivotal roles during this process. P-selectin–mediated rolling and α4β1 (VLA4)-VCAM-1 (vascular cell adhesion molecule-1)–mediated capture of encephalitogenic T cells on the brain endothelium is followed by αLβ2 (LFA-1)-ICAM-1/2 (intercellular adhesion molecule-1/2)–mediated T-cell polarization, crawling, and diapedesis (2). Once the T cells have passed the circulation, they become reprimed by antigen-presenting cells, which expose self-antigens of the myelin to further stimulate T-cell proliferation (3).

A hallmark of integrins is their ability to shift from an inactive to an active state (i.e. inside-out signalling), which is associated with an allosteric change of the integrin ectodomain and transmembrane domains and results in adhesion, sensing of substrate stiffness, and signal transduction (i.e. outside-in signalling) (4, 5). The allosteric modulation of the affinity state of integrins is regulated by talin and kindlin binding to the cytoplasmic domain of the β subunit (6) and is of particular importance for circulating platelets and leukocytes, which require fast attachment to blood vessel walls to seal leaks or react to inflammation. In addition to chemical allostery, integrin affinity also can be regulated by increasing the lifetime of integrin–ligand bonds, which can be achieved by integrin clustering, also known as avidity modulation (7, 8), and/or by application of tension (by, e.g., myosin II motors) to the adhesive bonds, resulting in the formation of catch bonds (9, 10). Whether kindlins are involved in bond lifetime regulation is not known.

Kindlins are evolutionary conserved and consist of three members (11). Hematopoietic cells express Kindlin-3 (11), the deletion of which in mice abrogates integrin activation, resulting in hemorrhages, leukocyte adhesion defects, and osteopetrosis (12–14). A human disease with similar abnormalities, leukocyte adhesion deficiency type III (LADIII), is also caused by null mutations of the *Kindlin-3* (*FERMT3*) gene (15–17). The severe LADIII defects lead to perinatal lethality, hindering the analysis of Kindlin-3 in specific blood cell lineages. We used conditional gene targeting to circumvent the problem of lethality and investigated the role of Kindlin-3 in effector T cells using EAE as model for T-cell–induced inflammation (18, 19). We report that autoreactive T cells lacking Kindlin-3 cannot extravasate and induce EAE when transferred into healthy mice. Interestingly, however, a high density of integrin ligands on inflamed vascular endothelial cells is sufficient to enable autoreactive T-cell extravasation and disease induction, and also to induce α4β1- and αLβ2-mediated effector T-cell adhesion and αLβ2-mediated crawling even under physiological shear conditions. These findings indicate that increased ligand concentrations can partially substitute Kindlin-3–mediated inside-out signaling, and that Kindlin-3 regulates both the activation of β1 and β2 integrins and the stabilization of integrin–ligand bonds.

Significance

T cells use integrins for adhesion to endothelial cells and extravasation. Thus, their blocking with Abs prevents T cell extravasation and ameliorates autoimmune diseases, such as multiple sclerosis (MS). Given the side effects of these Abs, we explored the integrin activator Kindlin-3 as potential therapeutic target. Mice lacking Kindlin-3 in T cells were immunized with an autoantigen to induce experimental autoimmune encephalitis (EAE), a model of MS. Although these mice developed EAE, adoptively transferred autoreactive T cells from Kindlin-3–deficient mice to healthy recipients failed to induce EAE. We found that autoreactive Kindlin-3–null T cells extravasate only when the brain microvasculature expresses high integrin ligand levels. Thus, blockage of Kindlin-3 is not a viable alternative approach to treating MS.

Author contributions: F.A.M., M.M., R.L., B.E., and R.F. designed research; F.A.M., M.M., R.L., M.A., and R.R. performed research; F.A.M., M.M., R.L., M.A., and R.R. analyzed data; and M.M. and R.F. wrote the paper.

The authors declare no conflict of interest.

This article is a PNAS Direct Submission.

[1]F.A.M. and M.M. contributed equally to this work.

[2]To whom correspondence should be addressed. E-mail: faessler@biochem.mpg.de.

This article contains supporting information online at www.pnas.org/lookup/suppl/doi:10.1073/pnas.1316032110/-/DCSupplemental.

Results

Kindlin-3 Is Not Required to Induce Active EAE. To analyze the role of Kindlin-3 in T cells, we backcrossed mice carrying a floxed Kindlin-3 gene 11 times with C57BL/6 mice (Kindlin-$3^{fl/fl}$, referred to as controls) and subsequently deleted the Kindlin-3 gene with C57BL/6 mice carrying the CD4Cre transgene (20). Western blot analysis demonstrated that $CD4^+$ and $CD8^+$ T cells isolated from the spleen of conditional Kindlin-$3^{fl/fl}$/CD4Cre (hereinafter, K3/Cre) mice lack Kindlin-3 expression (Fig. S1*A*). Kindlin-3 loss still allows the production of normal numbers of $CD4^+$ and $CD8^+$ T cells in the thymus, peripheral blood, and spleen of K3/Cre mice, suggesting that homeostatic T-cell proliferation, differentiation, and distribution in peripheral hematopoietic organs occur independent of Kindlin-3 (Fig. S1 *B*–*D*).

We next investigated whether effector T cells require Kindlin-3 for extravasation and induction of an inflammatory disease. To this end, we immunized mice with the encephalitogenic $MOG_{35–55}$ peptide to induce active EAE (aEAE) (19). K3/Cre mice and control littermates exhibited a similar EAE onset (Fig. 1*A*) with such clinical symptoms as weight loss (Fig. 1*B*) and paralysis (Fig. 1*C*). Immunostaining of the lumbar region of spinal cords revealed that diseased K3/Cre and control animals contained similar numbers of $CD45^{high}$ inflammatory cells and $CD45^{medium}$ microglial cells, Mac-1–positive monocytes/macrophages, and Gr-1-expressing granulocytes and macrophages. Furthermore, the subarachnoidal space and the spinal cord parenchyma of K3/Cre and control mice contained a comparable infiltrate of autoreactive $CD4^+$ T cells (Fig. 1*D*). Importantly, isotype control Ab staining verified the specificity of the immunostaining. FACS sorting of T cells from K3/Cre CNS infiltrates revealed normal numbers of $CD4^+$ T cells (Fig. S1*E*), and Western blot analysis confirmed the loss of Kindlin-3 expression (Fig. 1*E*). Taken together, these findings suggest that Kindlin-3–deficient T cells are able to extravasate and induce EAE.

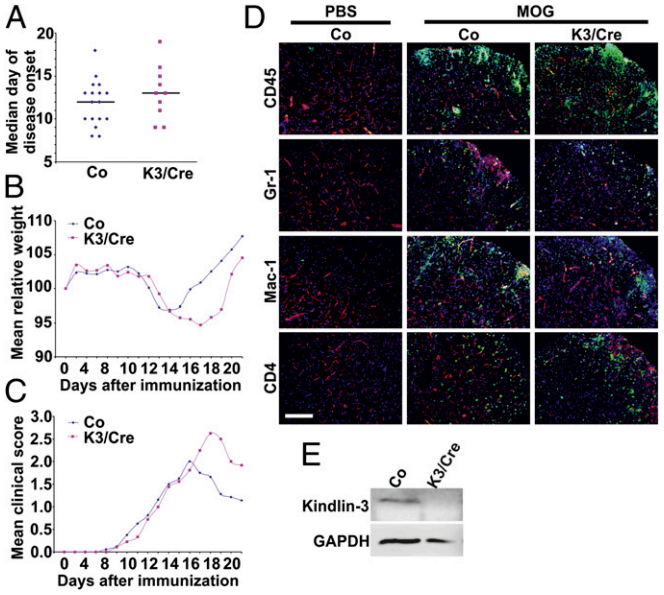

Fig. 1. aEAE in mice lacking Kindlin-3 expression in T cells. (*A*) Median day of disease onset in Kindlin-$3^{fl/fl}$/$CD4Cre^+$ (K3/Cre) and control (Co) mice with aEAE. (*B* and *C*) Relative weight normalized to day 0 (*B*) and clinical disease score (*C*) of mice with aEAE. Data points indicate means of 16 Co mice and 9 K3/Cre mice from two independent experiments. (*D*) Healthy control (PBS-treated) and diseased (MOG peptide-treated) mice with ongoing aEAE (clinical disease score 4) were killed, and spinal cord white matter was analyzed by immunostaining. Infiltrating leukocytes were stained with anti-CD45, anti-CD4, anti-Mac-1, or anti-Gr-1 Abs (green); blood vessels were stained with a pan-laminin Ab (red); and nuclei were stained with DAPI (blue). (Scale bar: 200 μm.) (*E*) Western blot analysis of protein lysates of FACS-sorted $CD4^+$ cells from the CNS of K3/Cre and Co mice with ongoing aEAE. GAPDH served as a loading control.

Kindlin-3 Is Required to Induce Passive EAE. The development of aEAE and the presence of Kindlin-3–deficient T cells in brain infiltrates of K3/Cre mice suggest that Kindlin-3 is not required for effector T-cell extravasation. To corroborate this finding, we tested whether Kindlin-3–deficient encephalitogenic T-cell blasts are able to induce passive EAE (pEAE) (18) in WT C57BL/6 mice. To this end, we crossed K3/Cre and littermate control mice with 2D2 mice, which express an MHC-II–restricted T-cell receptor (TCR) that specifically recognizes the $MOG_{35–55}$ peptide (21). We isolated naïve $CD4^+$ T splenocytes from Kindlin-$3^{fl/fl}$/$2D2^+$/$CD4Cre^+$ (hereinafter, $K3/Cre^{2D2}$) and control Kindlin-$3^{fl/fl}$/$2D2^+$ (hereinafter, Co^{2D2}) mice and primed them for several days in vitro with $MOG_{35–55}$-loaded dendritic cells (DCs) to induce proliferation and differentiation into memory (i.e., $CD62L^{hi}$/$CD44^{hi}$) and effector (i.e., $CD62L^{low}$/$CD44^{hi}$) T cells (Fig. 2*A*). The differentiated T-cell populations derived from $K3/Cre^{2D2}$ mice expressed normal levels of integrins and T-cell–specific maturation and activation markers (Fig. S2*A*), and lacked Kindlin-3 protein expression (Fig. 2*B*). Importantly, encephalitogenic T cells did not express α9β1 integrins (Fig. S2*B*), which can bind VCAM-1 as well.

To test whether Kindlin-3 affects T-cell differentiation into Th1, Th2, or Th17 cells, we performed intracellular FACS staining for IL-2, IFN-γ, TNF-α, IL-4, and IL-17. In these experiments, most Co^{2D2} and $K3/Cre^{2D2}$ cells were positive for IFN-γ and TNF-α, indicating that they are Th1-polarized rather than Th17-polarized (Fig. S2*C*). Consistent with the essential role of Kindlin-3 in integrin activation, resting and phorbol 12-myristate 13-acetate (PMA)-stimulated $K3/Cre^{2D2}$ effector T cells showed significantly reduced levels of 9EG7 epitope, which is induced in activated β1 integrins. Bypassing cellular activation by the addition of manganese resulted in comparable 9EG7 binding of Co^{2D2} and $K3/Cre^{2D2}$ effector T cells (Fig. S2*D*). Similarly, binding assays with soluble VCAM-1 revealed that both resting and PMA-stimulated $K3/Cre^{2D2}$ effector T cells bound significantly less VCAM-1 than control cells, which was rescued with manganese (Fig. S2*E*).

We next transferred the encephalitogenic T-cell blasts into sublethally irradiated WT C57BL/6 mice. As expected, the transfer of Co^{2D2} T-cell blasts induced EAE pathology with T-cell infiltration into the spinal cord, weight loss, and paralysis at approximately 11 d after the adoptive cell transfer (Fig. 2 *C*–*E*). Unexpectedly, however, none of the recipient mice that received $K3/Cre^{2D2}$ T-cell blasts developed EAE (Fig. 2 *C*–*E*), and in all recipients, Kindlin-3–deficient encephalitogenic $2D2^+$ T cells were detectable in the circulation for more than 3 wk after $K3/Cre^{2D2}$ T-cell transfer (Fig. S2*F*). Thus, in contrast to aEAE, the adoptive T-cell transfer experiments indicate that loss of Kindlin-3 protein in T-cell blasts prevents entry into a healthy CNS and thus induction of EAE.

Kindlin-3 Regulates Initial Arrest and Firm Adhesion to VLA-4 and LFA-1. Why can Kindlin-3–deficient encephalitogenic T cells enter the brain parenchyma to induce aEAE, but not pEAE? Induction of aEAE was achieved by immunization with antigens and the simultaneous treatment with complete Freund's adjuvant (CFA) and pertussis toxin (PT), which induces elevated expression of VCAM-1 and ICAM-1 on endothelial cells (Fig. 3 *A* and *B*) (22, 23). In contrast, in pEAE, T-cell blasts encounter naïve endothelial cells expressing low levels of ICAM-1 and VCAM-1. Thus, we hypothesized that high surface levels of endothelial cell adhesion molecules overcome compromised adhesive properties of Kindlin-3–deficient effector T cells and subsequent disease induction, whereas low integrin-ligand expression permits

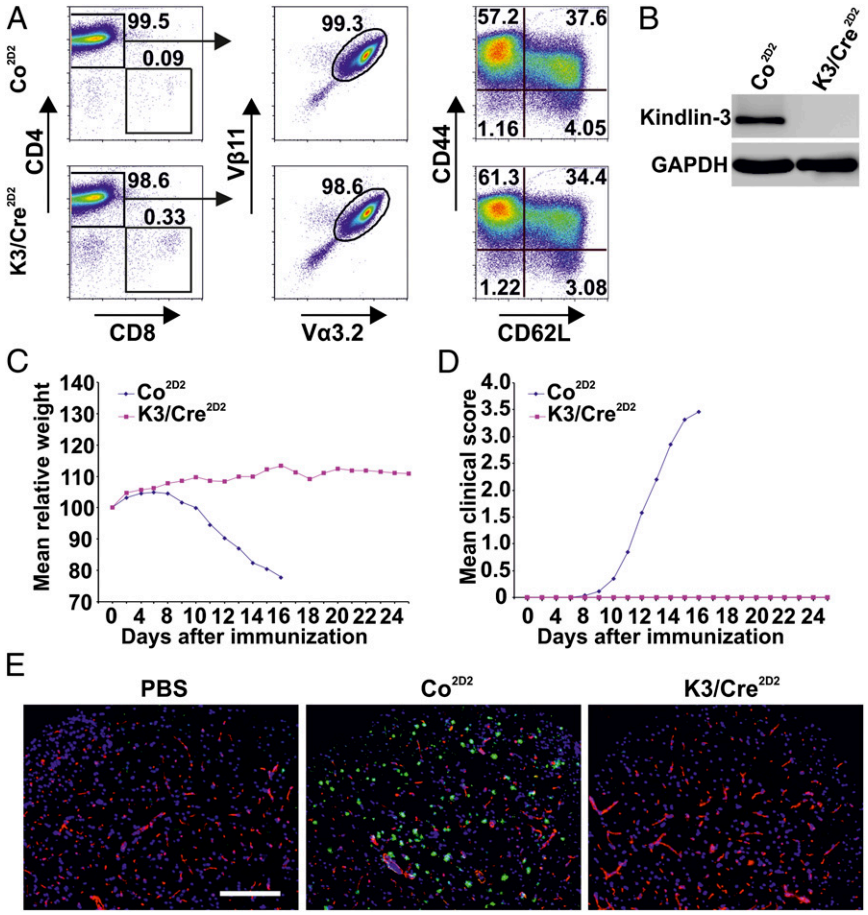

Fig. 2. Adoptively transferred autoreactive Kindlin-3–deficient T cells fail to induce EAE. (*A*) FACS analysis of in vitro-generated autoreactive T cells. Anti-CD4 and anti-CD8 Abs were used to identify $CD4^+$ T helper cells (*Left*), anti-Vα3.2 and anti-Vβ11 were used to identify $2D2^+$ cells (*Center*), and anti-CD62L and anti-CD44 were used to identify memory ($CD62L^{hi}/CD44^{hi}$) and effector ($CD62L^{low}/CD44^{hi}$) T cells (*Right*). (*B*) Western blot analysis of in vitro-primed and MACS-sorted Kindlin-$3^{fl/fl}/2D2^+/CD4Cre^+$ ($K3/Cre^{2D2}$) and control Kindlin-$3^{fl/fl}/2D2$ (Co^{2D2}) T cells. GAPDH served as a loading control. (*C* and *D*) Relative weight normalized to day 0 (*C*) and clinical disease score (*D*) of naïve WT C57BL/6 mice injected with encephalitogenic $K3/Cre^{2D2}$ and Co^{2D2} T cells. Data points represent means from three independent Co^{2D2} (n = 13) and $K3/Cre^{2D2}$ (n = 20) T-cell transfer experiments. (*E*) Immunostaining of the lumbar spinal cord white matter from C57BL/6 mice injected with either PBS or in vitro-generated encephalitogenic Co^{2D2} or $K3/Cre^{2D2}$ T cells. Infiltrating lymphocytes were stained with anti-CD4 Ab (green), blood vessels were stained with a pan-laminin Ab (red), and nuclei were stained with DAPI (blue). (Scale bar: 200 μm.)

adhesion and extravasation only after Kindlin-3–mediated integrin activation.

To test this hypothesis, we generated an inflamed, activated brain endothelium by inducing aEAE (clinical disease score 2) and injected either carboxyfluoresceine diacetate, succinimidyl ester (CFSE)-labeled Co^{2D2} or $K3/Cre^{2D2}$ T-cell blasts into the diseased mice. Immunohistology of spinal cords at 18 h after transfer revealed that Kindlin-3–null CFSE-labeled $CD4^+$ T cells, like WT cells, were indeed present in vessels, meninges, and brain parenchyma of these animals (Fig. 3 *C* and *D*). The quantification of CFSE-labeled T-cell numbers in spinal cord sections from mice injected with Co^{2D2} or $K3/Cre^{2D2}$ T-cell blasts revealed similar T-cell numbers in the spinal cord parenchyma (Fig. 3*E*).

To further validate whether the quantity of endothelial cell adhesion molecules can indeed modulate integrin-mediated adhesion of Kindlin-3–deficient effector T cells, we tested the flow-resistant binding of Co^{2D2} or $K3/Cre^{2D2}$ T-cell blasts to recombinant mouse VCAM-1 (rmVCAM-1) or recombinant mouse ICAM-1 (rmICAM-1) immobilized at different concentrations (24). In the same manner as for pEAE induction, T cells were isolated from spleen and lymph nodes and activated with MOG_{35-55}-loaded DCs. The activated T cells were allowed to accumulate on immunoglobulin cell adhesion molecules (IgCAMs) at very low shear forces (0.1 dyn/cm^2) and then exposed to an increased shear force of 1.5 dyn/cm^2 to wash away nonbound effector T cells (i.e., arrested T cells) and to assess for continuous shear-resistant firm adhesion (i.e., firmly adherent T cells). The numbers of arrested T cells per field of view (FOV) were counted when the laminar flow was reached at 15 s after shear enhancement, and the numbers of firmly adherent T cells per FOV were determined after 5, 10, and 15 min of continuous laminar flow. The experiments were controlled by coating the flow chambers with a nonintegrin ligand [100 nM Delta and Notch-like Epidermal growth factor-related Receptor precursor (DNER)-Fc] that demonstrated no T-cell adhesion. In agreement with our previous findings (25), Co^{2D2} T cells arrested and spread on immobilized rmVCAM-1 (Movie S1), but failed to crawl perpendicular and against the shear, which requires LFA-1–ICAM-1/2 interactions (25). The number of arrested Co^{2D2} T cells was approximately twofold higher than the number of $K3/Cre^{2D2}$ T cells on 100 nM rmVCAM-1 (Fig. 3*F*). The numbers of arrested Co^{2D2} and $K3/Cre^{2D2}$ T cells relative to the arrested T cells on 100 nM rmVCAM-1 decreased with decreasing concentrations (40 nM and 10 nM) of rmVCAM-1 (Fig. 3*G*). However, in relation to control cells, significantly fewer $K3/Cre^{2D2}$ T cells were arrested on 40 nM and 10 nM rmVCAM-1 (Fig. 3*G*). Notably, after exposure to physiological shear force on 100 nM rmVCAM-1 for 15 min, approximately 80% of the Co^{2D2} T cells remained firmly attached, whereas the proportion of firmly attached $K3/Cre^{2D2}$ T cells decreased to 60% after 5 min of continuous shear force and to 40% after 15 min of shear force (Fig. 3*H*). Thus, during continuous laminar flow, a significant number of $K3/Cre^{2D2}$ T cells maintained adhesive contact with rmVCAM-1, although at significantly lower numbers compared with Co^{2D2} T cells (Movie S2). Importantly, preincubation of T cells with an anti-α4β1 Ab blocked T-cell adhesion to VCAM-1, verifying the specificity of the T-cell interaction with rmVCAM-1.

We also analyzed LFA-1–mediated T-cell adhesion, polarity, and crawling on 10 nM, 40 nM, and 100 nM rmICAM-1 in flow experiments. The number of arrested Co^{2D2} T cells on 100 nM rmICAM-1 at 15 s after shear enhancement was fourfold higher than the numbers of $K3/Cre^{2D2}$ effector T cells (Fig. 3*I*).

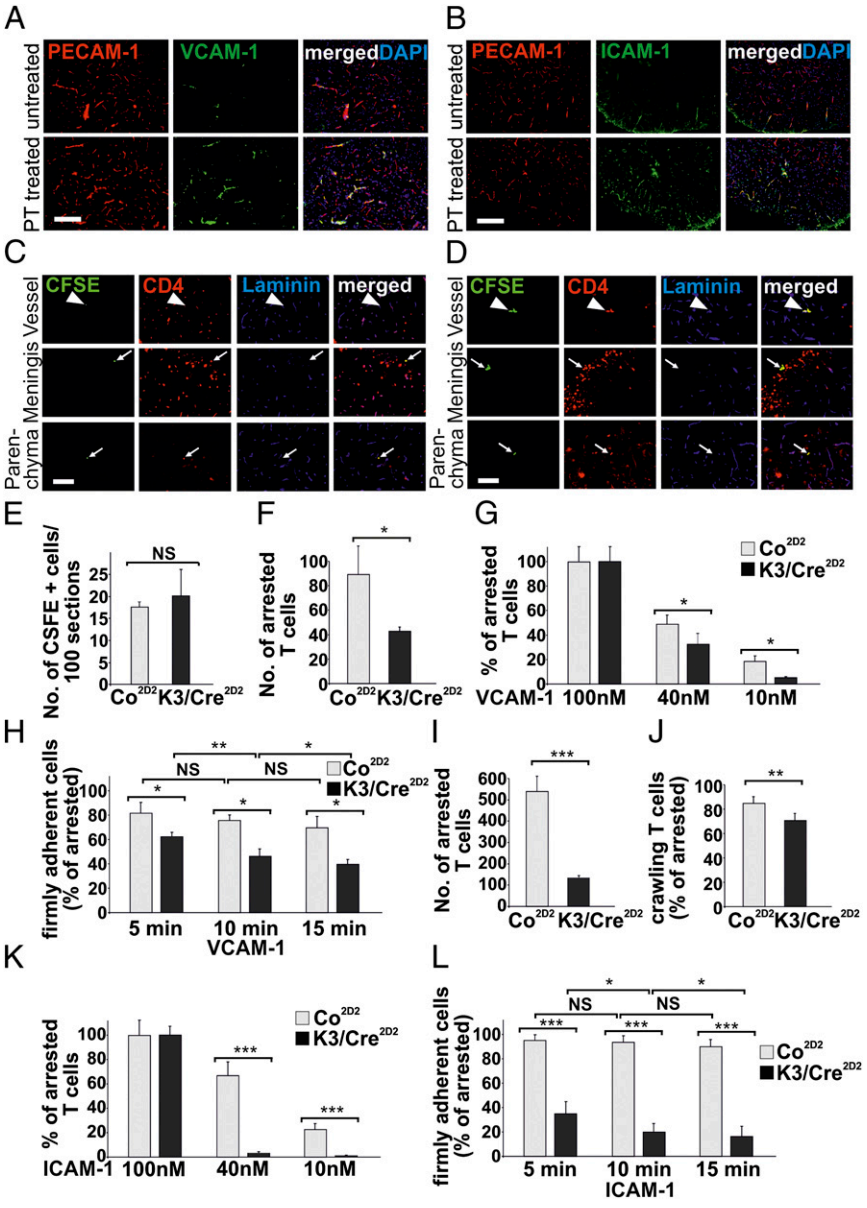

Fig. 3. Kindlin-3 controls firm adhesion of T cells to VCAM-1 and ICAM-1. (*A* and *B*) Spinal cords from untreated and pertussis toxin (PT)-treated animals were stained with anti–VCAM-1 (*A*) and anti–ICAM-1 (*B*) Abs (green). Blood vessels were stained with PECAM-1 Ab (red), and nuclei were stained with DAPI (blue). (Scale bar: 200 μm.) (*C* and *D*) Autoreactive CFSE$^+$-labeled (green) Co^{2D2} T cells (*C*) and K3/Cre^{2D2} T cells (*D*) injected into recipient C57BL/6 animals with ongoing aEAE (clinical disease score 2). Sections from lumbar spinal cords were stained with an anti-CD4 Ab (red) to identify infiltrating T lymphocytes. Blood vessels were stained with a pan-laminin Ab (blue). Arrowheads indicate CSFE$^+$ CD4$^+$ T cells within or in close proximity to blood vessels, and arrows indicate peripheral T cells in the parenchyma or meninges. (Scale bar: 100 μm.) (*E*) Numbers of CFSE$^+$-labeled Co^{2D2} and K3/Cre^{2D2} T cells in the lumbar region of the spinal cord at 18 h after transfer into mice with aEAE (clinical disease score 2). (*F*) Number of T cells arrested on surfaces coated with 100 nM rmVCAM-1 (n = 4 movies for Co; 4 movies for K3/Cre) per FOV. (*G*) Number of arrested T cells determined on surfaces coated with 100 nM (n = 4; 4), 40 nM (n = 4; 4), or 10 nM (n = 4; 4) rmVCAM-1, expressed as percent of arrested T cells on 100 nM VCAM-1. (*H*) Numbers of attached T cells determined at 5, 10 and 15 min of laminar flow at 1.5 dyn/cm^2, expressed as percent of arrested T cells determined at 15 s after shear increase. (*I*) Number of T cells arrested on surfaces coated with 100 nM rmICAM-1 (n = 4; 4). (*J*) Percentage of arrested T cells with crawling activity on 100 nM rmICAM-1 (n = 3; 3). (*K*) Number of arrested T cells determined on surfaces coated with 100 nM (n = 4; 4), 40 nM (n = 4; 4), and 10 nM (n = 4; 4) rmICAM-1 and expressed as percent of arrested T cells on 100 nM ICAM-1. (*L*) Percentage of firmly attached T cells on 100 nM (n = 3; 3) rmICAM-1. Numbers of attached T cells were determined at 5, 10, and 15 min of laminar flow at 1.5 dyn/cm^2 and expressed as percent of arrested T cells determined at 15 s after shear increase. *P < 0.05; **P < 0.01; ***P < 0.001; NS, not significant. Data are mean ± SD.

Interestingly, 85% of arrested Co^{2D2} effector T cells and 71% of arrested K3/Cre^{2D2} effector T cells rapidly polarized and began crawling on 100 nM rmICAM-1 (Fig. 3*J* and Movies S3 and S4). Although the proportions of arrested Co^{2D2} effector T cells were decreased on 40 nM and 10 nM rmICAM-1 (to 68% and 23%, respectively) almost no K3/Cre^{2D2} effector T cells were arrested on 40 nM and 10 nM ICAM-1 (4% and 2%, respectively) (Fig. 3*K*). After exposure to physiological shear force, 90% of Co^{2D2} T cells remained firmly attached during the entire 15-min shear force exposure, compared with only 18% of K3/Cre^{2D2} T cells (Fig. 3*L*). Treatment with an anti–LFA-1 Ab prevented adhesion of effector T cells to ICAM-1–coated flow chambers, underscoring the specificity of our assay.

Taken together, these findings indicate that high levels of VCAM-1 allow the arrest and adhesion of a significant number of Kindlin-3–deficient effector T cells under flow, whereas high levels of ICAM-1 enabled adhesion of a few Kindlin-3–deficient effector T cells, which polarized and crawled before they also finally detached.

T Cell Spreading and Adhesion on Brain Microvascular Endothelium Requires Kindlin-3. To investigate how Kindlin-3 affects effector T-cell adhesion and crawling in an ex vivo system, we performed live cell imaging with primary mouse brain microvascular endothelial cells (pMBMECs) (25, 26) stimulated with TNF-α to induce a proinflammatory phenotype with up-regulated expression of VCAM-1 and ICAM-1. After a flow chamber was mounted on the pMBMECs, the chamber was perfused with Co^{2D2} or K3/Cre^{2D2} T cells at low shear force (0.1 dyn/cm^2), to allow accumulation of T cells within a 4-min period. Subsequently, effector T cells were exposed to shear force (0.7 dyn/cm^2) for 10 min, and the interactions of dynamic effector T cells with the brain endothelium were imaged and quantified. The experiments revealed that after 15 s of shear force exposure, both Co^{2D2} T cells and K3/Cre^{2D2} T cells were able to arrest on activated endothelial cells and were immediately polarized (Movies S5 and S6); however, the number of arrested K3/Cre^{2D2} T cells was reduced to 48% of Co^{2D2} T cells (Fig. 4*A*). After 5 min and 10 min of laminar flow, the number of adherent K3/Cre^{2D2} T cells further decreased to 29% and 21%, respectively, whereas the number of

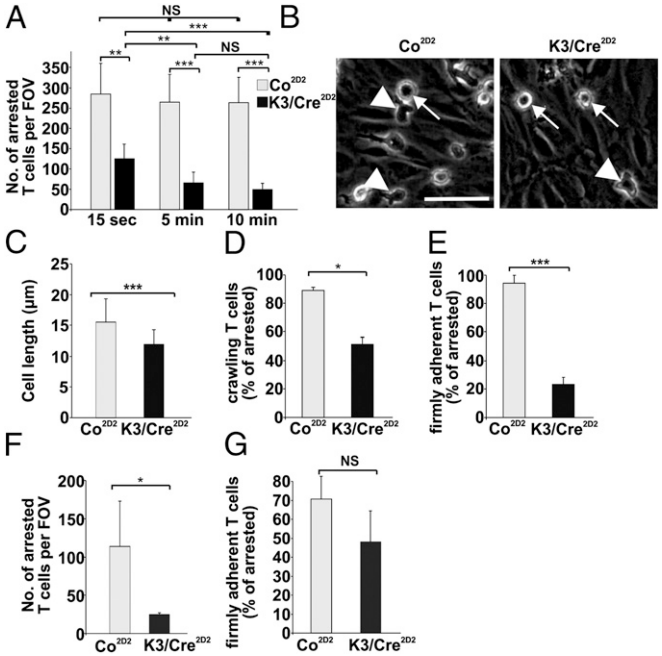

Fig. 4. Kindlin-3 promotes firm adhesion of T cells to primary brain microvascular endothelial cells. T-cell crawling and firm arrest on WT pMBMECs was analyzed by live cell imaging in a flow chamber experimental setup. (*A*) Numbers of arrested and firmly adherent T cells per FOV on WT pMBMECs determined 15 s, 5 min, and 10 min after onset of a 0.7-dyn/cm^2 shear (n = 7; 8). (*B*) Arrested K3/Cre^{2D2} T cells are more roundish and less polarized compared with Co^{2D2} T cells on WT pMBMECs. Arrows indicate stationary and more roundish cells, and arrowheads indicate polarized and migratory cells. (*C*) Mean cell lengths of Co^{2D2} and K3/Cre^{2D2} T cells (n = 105; 110). (*D*) Percentage of arrested (determined at 15 s after shear enhancement) Co^{2D2} and K3/Cre^{2D2} T cells with crawling activity on WT pMBMECs (n = 3 movies for Co; 3 movies for K3/Cre). (*E*) Percentage of arrested T cells able to resist 10 min of shear of 0.7 dyn/cm^2 on pMBMECs (n = 3; 3). (*F*) Number of arrested T cells per FOV on ICAM-1/-2 double KO pMBMECs at 15 s after onset of a 0.7-dyn/cm^2 shear (n = 4; 4). (*G*) Percentage of arrested T cells from ICAM-1/-2 double KO pMBMECs after 10 min of laminar flow at 0.7 dyn/cm^2 (n = 4; 4). *P < 0.05; **P < 0.01; ***P < 0.001. NS, not significant. Data are mean ± SD.

Co^{2D2} T cells remained unchanged (Fig. 4*A*). Although the adherent K3/Cre^{2D2} T cells polarized on the endothelial cell layer, this polarization was less efficient. Co^{2D2} T cells polarized and adopted a mean cell length of 15.50 ± 3.8 µm, whereas K3/Cre^{2D2} T cells polarized with a mean cell length of 11.9 ± 2.3 µm (Fig. 4 *B* and *C*). Importantly, approximately 50% of the adherent and polarized K3/Cre^{2D2} T cells initiated crawling on the brain endothelium before finally detaching within the 10 min of shear exposure (Fig. 4 *D* and *E*). Interestingly, flow chamber assays on TNF-α–treated pMBMECs isolated from ICAM-1^{null}/ICAM-2$^{-/-}$ mice (25) confirmed the important role of VCAM-1 (Fig. 3*E*) in the arrest and firm adhesion of K3/Cre^{2D2} T cells at 15 s after shear enhancement (Fig. 4*F*) and after 10 min of laminar flow (Fig. 4*G*).

Discussion

Inhibition of α4β1 with blocking Abs ameliorates the course of MS and thus has become a powerful therapy for MS (3). Likewise, genetic ablation of β1 in mice inhibits EAE (27), a widely used model for MS in rodents. Because EAE is triggered by autoreactive CD4$^+$ T cells, we used this model to examine the role of the integrin-activating adaptor protein Kindlin-3 for effector T-cell adhesion and crawling on brain endothelial cells, and to test whether Kindlin-3 is required to induce this inflammatory disease.

Stable integrin–ligand interactions require the conversion of the integrin conformation toward a high-affinity state and the subsequent stabilization of integrin–ligand bonds (4, 6). Consequently, it can be assumed that a loss of integrin activation in autoreactive T cells should abrogate α4β1 function and thus also prevent EAE. In line with this expectation, transfer of autoreactive T cells lacking the essential integrin activator Kindlin-3 prevented the development of EAE in recipient mice. In sharp contrast to these findings, however, Kindlin-3–deficient T cells efficiently induced active EAE, despite efficient and complete Kindlin-3 gene deletion. A likely explanation for the different outcomes is the different integrin ligand levels expressed on endothelial cells at the time of EAE induction. This hypothesis is supported by the efficient extravasation of adoptively transferred Kindlin-3–deficient effector T-cell blasts into an inflamed brain that expresses high levels of VCAM-1 and ICAM-1 on endothelial cells.

Why are Kindlin-3–deficient T-cell blasts able to adhere, arrest, and extravasate at sites of high integrin–ligand expression, despite their reduced VCAM-1 and 9EG7 binding? Our flow chamber experiments revealed that Kindlin-3–deficient effector T cells can adopt an affinity state for α4β1 integrin that allows remarkably efficient T-cell capture and transient arrest on recombinant VCAM-1. In contrast, transient effector T-cell adhesion to recombinant ICAM-1 was much more strongly impaired, indicating that αLβ2 integrins critically depend on Kindlin-3 for adoption of a high-affinity state. Interestingly, however, increasing levels of VCAM-1 as well as ICAM-1 increased the arrest of Kindlin-3–deficient effector T cells under shear force. Despite this efficient arrest of Kindlin-3–deficient effector T cells at high VCAM-1 levels, firm adhesion on recombinant VCAM-1 and endothelial cells was reduced. These findings are in line with a previous report showing that chemokine-stimulated Kindlin-3–deficient LAD-III effector T cells show transient adhesion, but not stable adhesion, to VCAM-1 under flow conditions (28). Furthermore, these findings suggest that α4β1 on Kindlin-3–deficient effector T cells can adopt an affinity state sufficient for the production of weak α4β1–VCAM-1 interactions. The number of weak α4β1–VCAM-1 interactions on activated brain endothelial cells may increase to a level that enables sufficient numbers of T-cell blasts to firmly adhere, extravasate, and induce disease.

A similar mechanism also operates with αLβ2 on Kindlin-3–deficient effector T cells and has been suggested for Kindlin-3–deficient neutrophils, on which αLβ2 can adopt an intermediate conformation allowing slow leukocyte rolling on endothelial cells (29). This intermediate conformation of αLβ2 requires Talin-1, suggesting that the initial contact with ICAM-1 is Kindlin-3–independent, whereas further conformational changes associated with the high-affinity state are Kindlin-3–dependent (29). A similar finding also has been reported for αIIbβ3 integrin binding to fibrinogen, which occurs in the presence of Talin-1 alone (30).

A further striking finding of the present study is that a small but significant number of Kindlin-3–deficient T cells adhered to recombinant ICAM-1– or TNF-α–treated endothelial cells and began to polarize and crawl, albeit less efficiently than WT T cells. This clearly indicates that β2 integrins induce outside-in signals even in the absence of Kindlin-3 and before reaching a fully active conformation. In contrast, the majority of Kindlin-3–deficient T cells attached to VCAM-1, ICAM-1, or TNF-α–treated endothelial cells are unable to resist higher shear forces, indicating that strengthening of integrin interactions with these ligands requires further changes in α4β1 and αLβ2 that are mediated by Kindlin-3 (31, 32). It is possible that these changes represent conformational changes of the integrin ectodomain induced by tension and resulting in the formation of catch bonds that increase bond lifetimes. It is also possible that Kindlin-3 increases bond lifetimes by clustering integrins, thereby enabling avidity that combines the strength of multiple integrin–ligand bonds (33). The mechanism regulated by Kindlin-3, and whether

this pathway can be exploited to combat inflammation, remain to be identified and tested.

Materials and Methods

Animals. Kindlin-3 floxed (Kindlin-3$^{fl/fl}$) mice, in which exons 3–6 of the Kindlin-3 gene is flanked with loxP sites, were backcrossed more than 11 times with C57BL/6 mice, then intercrossed with C57BL/6 mice carrying a CD4 promoter-driven Cre recombinase transgene (20). To obtain $MOG_{35–55}$-specific TCR transgenic mice deficient for the Kindlin-3 gene, Kindlin-3$^{fl/fl}$/CD4Cre^{+} mice were intercrossed with 2D2 transgenic mice (21). All mice were bred in the animal facilities at the Max Planck Institute of Biochemistry. All EAE experiments were performed in accordance with the license of the government of Oberbayern.

Induction of aEAE and pEAE. aEAE was induced by s.c. administration of $MOG_{35–55}$ peptide as described previously (34). pEAE was induced by an i.v. transfer of 2×10^6 encephalitogenic T cells into WT sex-matched C57BL/6 mice sublethally irradiated with 3.5 Gy. To obtain encephalitogenic T cells, spleen and axillary, brachial, inguinal, and paraaortal lymph nodes were isolated from Kindlin-3$^{fl/fl}$/2D2^{+}/CD4Cre^{+} and control Kindlin-3$^{fl/fl}$/2D2^{+} mice. Single-cell suspensions were obtained, and after ammonium-chloride-potassium lysis of RBCs, cells from two mice were cocultured with 4×10^6 DCs loaded for 2 h with 20 μg/mL $MOG_{35–55}$ peptide. After 4 d of coculture, the cell suspensions were split 1:2 into medium containing 5 ng/mL IL-2 (R&D Systems). After another 6 d of culture, dead cells were removed by density gradient centrifugation (Nycoprep 1.077; Axis-Shield). A total of 2×10^6 cells per well were incubated overnight in 24-well plates coated with 1 μg/mL anti-mouse CD3e and CD28 Abs (both from eBioscience) and in the presence of recombinant murine IL-18 (20 ng/mL; MBL) and IL-12 (25 ng/mL) and IL-23 (10 ng/mL; both from R&D Systems). The cells were then washed three times with PBS and transferred i.v. into recipient mice. Clinical disease score and weight of the mice with aEAE and transfer EAE were checked daily. Scoring of the mice was as follows: 0, healthy; 1, limp tail; 2, hind leg weakness; 3, one paralyzed hind leg; 4, two paralyzed hind legs; 5, moribund.

Live Cell Imaging Under Flow Conditions. Live cell imaging on TNF-α–stimulated pMBMECs isolated from WT or ICAM-1^{null}/ICAM-2$^{-/-}$ C57BL/6 mice, or on immobilized recombinant mouse ICAM-1 (rmICAM-1), VCAM-1 (rmVCAM-1), or DNER (rmDNER; all from R&D Systems) was performed as described previously (25, 26). CD3e- and CD28-activated T cell blasts (2×10^6/mL) were allowed to accumulate for 3–4 min at low shear force (0.1 dyn/cm^2). Then, dynamic T cell interactions with pMBMECs or immobilized rmICAM-1 and rmVCAM-1 were recorded under physiological shear force (1.5 dyn/cm^2) for 15 s (defined as arrested T cells) and for 5, 10, and 15 min (defined as firmly adherent T cells). Specific integrin-mediated adhesion to ICAM-1 and VCAM-1 was tested by pretreating T cells with rat mAbs specific for mouse α4 integrin (PS/2) and mouse LFA-1 (FD448.1). An anti-human CD44 (9B5) Ab was used as negative control. All Abs were incubated with the T cells for 20 min at a concentration of 10 μg/mL

Flow Cytometry. Single-cell suspensions of hematopoietic organs were prepared and staining for FACS analysis was done as described previously (34) and detailed in *SI Materials and Methods*. For intracellular cytokine stainings, T-cell blasts were stimulated for 4 h with 50 ng/mL PMA, 500 ng/mL ionomycin, and 10 μg/mL brefeldin A (Sigma-Aldrich), and cytokine expression was analyzed as described previously (27).

For analysis of soluble VCAM-1–Fc binding, 0.5×10^6 effector T cells were incubated with 100 μg/mL VCAM-Fc (R&D Systems) for 15 min at 37 °C in HBSS binding media supplemented with 0.2% BSA, Ca^{2+} and Mg^{2+} (1 mM each), Mn^{2+} (2 mM), or PMA (100 ng/mL). Cells were then washed once, incubated with PE-donkey anti-human IgG (Jackson ImmunoResearch) for an additional 20 min on ice, washed twice, and analyzed by FACS.

Statistical Analysis. Means, SDs, and statistical comparisons with the Student *t* test (*$P < 0.05$; **$P < 0.01$; ***$P < 0.001$) were performed using Microsoft Excel software.

ACKNOWLEDGMENTS. We thank Michal Grzejszczyk, Claudia Blatti, and Mark Liebi for expert technical assistance; Kevin Flynn for a careful read of the manuscript; and the Microscopy Imaging Center of the University of Bern for support. The work was supported by the Swiss National Science Foundation (Grant 31003A_149420, to B.E. and R.L.), the Deutsche Forschugsgemeinschaft (Grant SFB914, to M.M. and R.F.), and the Max Planck Society (R.F.).

1. McFarland HF, Martin R (2007) Multiple sclerosis: A complicated picture of autoimmunity. *Nat Immunol* 8(9):913–919.
2. Engelhardt B (2010) T cell migration into the central nervous system during health and disease: Different molecular keys allow access to different central nervous system compartments. *Clin Exp Neuroimmunol* 1:79–93.
3. Steinman L (2005) Blocking adhesion molecules as therapy for multiple sclerosis: Natalizumab. *Nat Rev Drug Discov* 4(6):510–518.
4. Hynes RO (2002) Integrins: Bidirectional, allosteric signaling machines. *Cell* 110(6):673–687.
5. Kim C, Ye F, Ginsberg MH (2011) Regulation of integrin activation. *Annu Rev Cell Dev Biol* 27:321–345.
6. Moser M, Legate KR, Zent R, Fässler R (2009) The tail of integrins, talin, and kindlins. *Science* 324(5929):895–899.
7. Kinashi T (2005) Intracellular signalling controlling integrin activation in lymphocytes. *Nat Rev Immunol* 5(7):546–559.
8. Paszek MJ, Boettiger D, Weaver VM, Hammer DA (2009) Integrin clustering is driven by mechanical resistance from the glycocalyx and the substrate. *PLOS Comput Biol* 5(12):e1000604.
9. Kong F, García AJ, Mould AP, Humphries MJ, Zhu C (2009) Demonstration of catch bonds between an integrin and its ligand. *J Cell Biol* 185(7):1275–1284.
10. Marshall BT, et al. (2003) Direct observation of catch bonds involving cell-adhesion molecules. *Nature* 423(6936):190–193.
11. Ussar S, Wang HV, Linder S, Fässler R, Moser M (2006) The Kindlins: Subcellular localization and expression during murine development. *Exp Cell Res* 312(16):3142–3151.
12. Moser M, et al. (2009) Kindlin-3 is required for beta2 integrin-mediated leukocyte adhesion to endothelial cells. *Nat Med* 15(3):300–305.
13. Moser M, Nieswandt B, Ussar S, Pozgajova M, Fässler R (2008) Kindlin-3 is essential for integrin activation and platelet aggregation. *Nat Med* 14(3):325–330.
14. Schmidt S, et al. (2011) Kindlin-3–mediated signaling from multiple integrin classes is required for osteoclast-mediated bone resorption. *J Cell Biol* 192(5):883–897.
15. Kuijpers TW, et al. (2009) LAD-1/variant syndrome is caused by mutations in *FERMT3*. *Blood* 113(19):4740–4746.
16. Malinin NL, et al. (2009) A point mutation in *KINDLIN3* ablates activation of three integrin subfamilies in humans. *Nat Med* 15(3):313–318.
17. Svensson L, et al. (2009) Leukocyte adhesion deficiency-III is caused by mutations in *KINDLIN3* affecting integrin activation. *Nat Med* 15(3):306–312.
18. Stromnes IM, Goverman JM (2006) Passive induction of experimental allergic encephalomyelitis. *Nat Protoc* 1(4):1952–1960.
19. Stromnes IM, Goverman JM (2006) Active induction of experimental allergic encephalomyelitis. *Nat Protoc* 1(4):1810–1819.
20. Lee PP, et al. (2001) A critical role for Dnmt1 and DNA methylation in T cell development, function, and survival. *Immunity* 15(5):763–774.
21. Bettelli E, et al. (2003) Myelin oligodendrocyte glycoprotein-specific T cell receptor transgenic mice develop spontaneous autoimmune optic neuritis. *J Exp Med* 197(9):1073–1081.
22. Bergman RK, Munoz JJ, Portis JL (1978) Vascular permeability changes in the central nervous system of rats with hyperacute experimental allergic encephalomyelitis induced with the aid of a substance from *Bordetella* pertussis. *Infect Immun* 21(2):627–637.
23. Steffen BJ, Butcher EC, Engelhardt B (1994) Evidence for involvement of ICAM-1 and VCAM-1 in lymphocyte interaction with endothelium in experimental autoimmune encephalomyelitis in the central nervous system in the SJL/J mouse. *Am J Pathol* 145(1):189–201.
24. Constantin G, et al. (2000) Chemokines trigger immediate beta2 integrin affinity and mobility changes: Differential regulation and roles in lymphocyte arrest under flow. *Immunity* 13(6):759–769.
25. Steiner O, et al. (2010) Differential roles for endothelial ICAM-1, ICAM-2, and VCAM-1 in shear-resistant T cell arrest, polarization, and directed crawling on blood-brain barrier endothelium. *J Immunol* 185(8):4846–4855.
26. Coisne C, Lyck R, Engelhardt B (2013) Live cell imaging techniques to study T cell trafficking across the blood–brain barrier in vitro and in vivo. *Fluids Barriers CNS* 10(1):7.
27. Bauer M, et al. (2009) Beta1 integrins differentially control extravasation of inflammatory cell subsets into the CNS during autoimmunity. *Proc Natl Acad Sci USA* 106(6):1920–1925.
28. Manevich-Mendelson E, et al. (2009) Loss of Kindlin-3 in LAD-III eliminates LFA-1 but not VLA-4 adhesiveness developed under shear flow conditions. *Blood* 114(11):2344–2353.
29. Lefort CT, et al. (2012) Distinct roles for talin-1 and kindlin-3 in LFA-1 extension and affinity regulation. *Blood* 119(18):4275–4282.
30. Ye F, et al. (2010) Recreation of the terminal events in physiological integrin activation. *J Cell Biol* 188(1):157–173.
31. Hao JJ, et al. (2008) Enrichment of distinct microfilament-associated and GTP-binding proteins in membrane/microvilli fractions from lymphoid cells. *J Proteome Res* 7(7):2911–2927.
32. Hyduk SJ, et al. (2011) Talin-1 and kindlin-3 regulate alpha4beta1 integrin-mediated adhesion stabilization, but not G protein-coupled receptor-induced affinity up-regulation. *J Immunol* 187(8):4360–4368.
33. Feng C, et al. (2012) Kindlin-3 mediates integrin αLβ2 outside-in signaling, and it interacts with scaffold protein receptor for activated-C kinase 1 (RACK1). *J Biol Chem* 287(14):10714–10726.
34. Montanez E, et al. (2007) Analysis of integrin functions in peri-implantation embryos, hematopoietic system, and skin. *Methods Enzymol* 426:239–289.